

Spectral energy transport in two-dimensional quantum vortex dynamics

T. P. Billam,^{1,2,*} M. T. Reeves,¹ and A. S. Bradley^{1,†}

¹Jack Dodd Centre for Quantum Technology, Department of Physics, University of Otago, Dunedin 9016, New Zealand

²Joint Quantum Centre (JQC) Durham–Newcastle, Department of Physics, Durham University, Durham, DH1 3LE, UK

(Dated: October 16, 2018)

We explore the possible regimes of decaying two-dimensional quantum turbulence, and elucidate the nature of spectral energy transport by introducing a dissipative point-vortex model with phenomenological vortex-sound interactions. The model is valid for a large system with weak dissipation, and also for systems with strong dissipation, and allows us to extract a meaningful and unambiguous spectral energy flux associated with quantum vortex motion. For weak dissipation and large system size we find a regime of hydrodynamic vortex turbulence in which energy is transported to large spatial scales, resembling the phenomenology of the transient inverse cascade observed in decaying turbulence in classical incompressible fluids. For strong dissipation the vortex dynamics are dominated by dipole recombination and exhibit no appreciable spectral transport of energy.

PACS numbers: 03.75.Lm 67.85.De 47.27.-i

I. INTRODUCTION

Classical two-dimensional (2D) turbulence exhibits a well-established universal phenomenology of spectral scaling laws and energy transport, where energy is conservatively transported to large scales through a lossless inertial range, a process known as the inverse energy cascade [1, 2]. While the Kolmogorov $-5/3$ power law associated with an inertial range has been observed in simulations of two-dimensional quantum turbulence (2DQT) in the context of dilute gas Bose-Einstein condensates (BECs) [3, 4], the nature of spectral energy transport in 2DQT remains a crucial open question, with recent studies conflicting over whether energy is transported to large [4–6] or small [7, 8] scales. As a model of a compressible superfluid, the 2D Gross-Pitaevskii equation (GPE) can simultaneously support several regimes of turbulence, including weak wave turbulence [9–11], negative temperature point-vortex states in decaying [5, 6] and forced [4, 12, 13] quantum turbulence, and evolution near non-thermal fixed points [14–16], offering a rich phenomenology involving coupled quantum vortex and classical wave degrees of freedom.

The major challenge for understanding spectral energy transport in 2DQT is the difficulty in identifying an unambiguous measure of spectral energy flux in a superfluid that is compressible and, in general, dissipative [8, 17]. Previous identifications of turbulent cascades have relied on a combination of a spectral $k^{-5/3}$ scaling region and an indirect measure of energy flux, such as vortex clustering and spectral energy condensation [4], energy flux through black-hole horizons in a holographic gravity dual [7], or other approximate methods [8], all of which are unable to unambiguously distinguish the conservative transfer of vortex energy between spatial scales from the loss of vortex energy due to the coupling to compressible degrees of freedom. Furthermore, 2DQT studies

have addressed systems for which the importance of vortex-sound interactions varies greatly, leading to quite different results. This diversity motivates a systematic exploration of the important physical processes in regimes of 2DQT.

Here, we identify regimes of decaying 2DQT within GPE theory by varying the system size and dissipation rate for a given initial condition, allowing systematic control over the importance of vortex-sound interactions. To study the role of energy transport in the different regimes we introduce a dissipative point-vortex model for quantum vortices, to which we add phenomenological vortex-sound interactions. This model allows us to extract an unambiguous spectral energy flux and analyze the effects of dissipation. The model agrees well with the damped, projected Gross-Pitaevskii equation (dPGPE), a physically well-justified model of BECs [18], both for large system sizes and for strong dissipation. We find that for large system sizes and weak dissipation relevant to BEC experiments [12], as explored in Ref. [5], energy is indeed transported to large scales by vortex interactions. We find time-averaged spectral characteristics broadly consistent with the phenomenology of decaying turbulence in a classical incompressible fluid [19], including an approximately lossless inertial range with negative spectral energy flux. We term this phenomenological regime *hydrodynamic vortex turbulence*.

In the cases of strong dissipation, and weak dissipation in a small system, this phenomenology is replaced by a dissipative collapse of the spectrum, driven by the formation of vortex dipoles and rapid vortex-antivortex annihilation. While our effective point-vortex model does not accurately describe the dPGPE dynamics in the small system with weak dissipation (where dominant vortex-sound interactions place the system in a strong wave-turbulent regime), the long-time evolution in all these cases appears similar to dynamics generated by the non-thermal fixed point identified in previous classical field studies [14–16]. This corresponds to a low-energy, long-lived configuration of a small number of vortices, arranged in vortex dipoles. In contrast to the regime of hydrodynamic vortex turbulence, the vortex dynamics in these cases is found to lack any significant spectral transport of energy through scale space, and has no direct analogue in classical fluid turbulence.

* Author to whom correspondence should be addressed; Email: thomas.billam@durham.ac.uk

† Author to whom correspondence should be addressed; Email: abradley@physics.otago.ac.nz

II. GROSS-PITAEVSKII MODEL

We model a finite-temperature BEC using the two-dimensional dPGPE [18]

$$i\hbar \frac{\partial \psi(\mathbf{r}, t)}{\partial t} = (1 - i\gamma) \mathcal{P}_c \{ (\mathcal{L}[\mathbf{r}, \psi(\mathbf{r}, t)] - \mu) \psi(\mathbf{r}, t) \}, \quad (1)$$

where $\mathcal{L}[\mathbf{r}, \psi(\mathbf{r}, t)] = -\hbar^2 \nabla_{\perp}^2 / 2m + g_2 |\psi(\mathbf{r}, t)|^2$, we have assumed oscillator length $l_z = \sqrt{\hbar/m\omega_z}$, corresponding to tight harmonic confinement in the z -direction, and $g_2 = \sqrt{8\pi} \hbar^2 a_s / ml_z$, where m is the atomic mass, a_s the s -wave scattering length, and μ the chemical potential. The projector \mathcal{P}_c ensures complete numerical dealiasing within our pseudospectral integration method [5, 21]. The dimensionless damping rate γ describes thermal dissipative collisions between condensate atoms and non-condensate atoms; this is an important physical effect in atomic superfluids, and has proved useful as both a qualitative and semi-quantitative model for 2DQT experiments [3, 22, 23].

We enumerate the regimes of decaying 2DQT by using Eq. (1) to simulate the decay of a periodic lattice of unstable charge-six ($\kappa_i = \pm 6$) vortices, similar to Ref. [7]. We work in a periodic square box of length $L\xi$ where $\xi = \hbar/\sqrt{\mu m}$ is the healing length, and vary the parameters L and γ ; representative results are shown in Fig. 1 [20]. In all cases the $\kappa_i = \pm 6$ vortices rapidly disintegrate, forming a negative-temperature vortex state with high point-vortex energy [5]. This state subsequently evolves in different ways, depending primarily on the system size and dissipation rate.

In the case of high dissipation [$\gamma = 10^{-1}$, Fig. 1(a,b)] the strong dissipation rapidly removes compressible energy for all box sizes L . The system also loses large amounts of vortex energy, and large numbers of vortices to pair annihilation, and evolves toward a long-lived, low-energy configuration of relatively few vortices. For weaker, experimentally relevant, dissipation [$\gamma = 10^{-5}$] and a small box size $L = 175$, the initial disintegration of the $\kappa_i = \pm 6$ vortices releases compressible kinetic energy comparable to the incompressible kinetic energy carried by the vortices, and the resulting strong coupling between sound and vortices leads to a regime of strong wave turbulence [Fig. 1(d,i)]. However, at later times the sound and vortex degrees of freedom cease to interact as strongly, and we observe a long-lived configuration of few vortices arranged as dipoles, similar to those observed for high dissipation in cases (a) and (b). As discussed in Ref. [24], these positive-temperature configurations of few vortices have no direct analogue in developed classical fluid turbulence.

For weaker dissipation applicable to BEC experiments [$\gamma = 10^{-5}$] and a *large* box size [$L = 700$] the initial incompressible kinetic energy dominates the compressible kinetic energy released by disintegration of the $\kappa_i = \pm 6$ vortices [Fig. 1(c)]. The subsequent high-energy vortex dynamics, largely unaffected by dissipation or vortex-sound interactions, are qualitatively different to the other cases. In this regime of *hydrodynamic vortex turbulence* one appears to recover the transport of kinetic energy to large scales expected in classical 2D turbulence [1, 2, 19] and reported in Refs. [5, 6, 12, 25].

III. DISSIPATIVE POINT-VORTEX MODEL

The N -vortex solutions of Eq. (1) with approximately uniform background density and well-separated vortex cores can be described by a point-vortex model [26]. Here, we develop such a model in order to gain significant insights into the general dynamical regimes outlined above. Our model includes the effects of dissipation due to γ directly, and the effects of coupling to sound phenomenologically. Note that from here on, we will focus on cases (a), (b), and (c), as in case (d) strong density fluctuations preclude a quantitative description of the early-time dynamics in terms of point-vortices. The later evolution of case (d) may be describable in terms of a point-vortex model with a phenomenologically altered value of γ , but we will not pursue this possibility here.

In the presence of dissipation, the general equation of motion for the i th vortex, located at \mathbf{r}_i and with charge $\kappa_i = \pm 1$ (circulation $\kappa_i \hbar/m$), is [27]

$$\frac{d\mathbf{r}_i}{dt} = \frac{\hbar}{m} (\nabla \theta|_{\mathbf{r}=\mathbf{r}_i} - \gamma \kappa_i \hat{\mathbf{e}}_3 \times \nabla \theta|_{\mathbf{r}=\mathbf{r}_i}), \quad (2)$$

where θ is the phase of the wavefunction, and $\hat{\mathbf{e}}_3$ is a unit vector in the z -direction. This leads to the dissipative point-vortex model

$$\frac{d\mathbf{r}_i}{dt} = \mathbf{v}_i + \mathbf{w}_i; \quad \mathbf{v}_i = \sum_{j=1}^{N'} \mathbf{v}_i^{(j)}; \quad \mathbf{w}_i = -\gamma \kappa_i \hat{\mathbf{e}}_3 \times \mathbf{v}_i, \quad (3)$$

where the primed summation indicates omission of the term $j = i$, and we have explicitly separated the velocity of the i th vortex into a Hamiltonian part, \mathbf{v}_i , and a dissipative (Peach-Koehler [28]) part, \mathbf{w}_i . Hence, $\mathbf{v}_i^{(j)}$ represents the velocity of the i th vortex due to the j th in a Hamiltonian point-vortex model with appropriate boundary conditions. We consider a periodic square domain of size $L\xi \times L\xi$, in which case [29]

$$\mathbf{v}_i^{(j)} = \frac{\pi c \kappa_j}{L} \sum_{m=-\infty}^{\infty} \left(\frac{-\sin(y'_{ij})}{\cosh(x'_{ij} - 2\pi m) - \cos(y'_{ij})} \right), \quad (4)$$

where $(x_{ij}, y_{ij}) \equiv \mathbf{r}_{ij} \equiv \mathbf{r}_i - \mathbf{r}_j$, $(x'_{ij}, y'_{ij}) = 2\pi(x_{ij}, y_{ij})/L\xi$, and $c = \sqrt{\mu/m}$ is the speed of sound.

The coupling between incompressible and compressible energy in an atomic BEC introduces physics not captured by Eq. (3) primarily when vortices approach close to, or within, core-overlap distances. We therefore phenomenologically account for these effects within our model in two ways: Firstly, similarly to Refs. [6, 24], we remove vortex dipoles in which the constituent vortices approach each other within one healing length ξ . This mimics the vortex-antivortex annihilations that can be a key feature of quantum turbulence in compressible superfluids [6, 17, 30]. Secondly, we modify the dissipation γ for vortices with nearby same-sign neighbours, replacing γ in Eq. (3) with

$$\gamma_i = \max \left(\exp \left[\ln(\gamma) \frac{r_{is} - r_1}{r_2 - r_1} \right], \gamma \right), \quad (5)$$

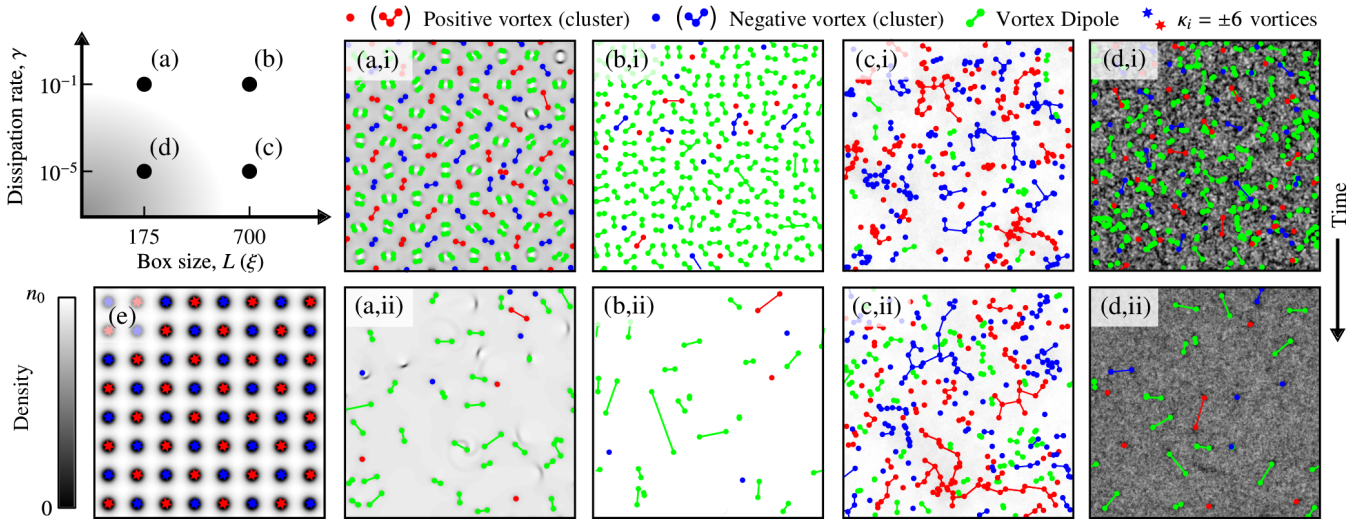


FIG. 1. (Color online) Regimes of decaying 2DQT following the decay of an unstable lattice of charge $\kappa_i \pm 6$ vortices, computed using the dPGPE (see also [20]). We show schematically the effects of dimensionless dissipation rate, γ , and box size, L , (see axes, top left) on the dynamics: We show the density (grayscale, background) and vortex configuration analyzed with the recursive cluster algorithm [4] (see key) at both short (i) and long (ii) times after the break-up of the lattice, compared to the characteristic timescale of the dynamics. In (e) we show the initial lattice for $L = 175$. The regimes can be characterised as dissipative dipole gas dynamics (a,b), hydrodynamic vortex turbulence with energy transport to large scales (c), and strong wave turbulence with close vortex-sound coupling (d) [indicated schematically on axes (top left) by shaded region].

where r_{is} is the distance to the nearest same-sign neighbour of vortex i , $r_2 = 10\xi$, and $r_1 = \xi$. This phenomenologically accounts for radiation of sound by rapidly-accelerating vortices, an effect for which an approximate analytic treatment exists for an isolated vortex pair [31, 32], but would appear to be impractical for general N -vortex configurations. In practice, we find that our phenomenological model captures the important physics of radiation while remaining reasonably insensitive to variations in r_1 and r_2 around our chosen values.

IV. SPECTRAL ANALYSIS

Using our phenomenological point-vortex model, we simulate ensembles of 10 trajectories in a scenario similar to Fig. 1 for 15–20 turnover times $\tau \equiv L\xi/u_{\text{rms}}$, where u_{rms} is the average root-mean square velocity over the ensemble at $t = 0$. The ensemble is defined by beginning from configurations in which six appropriately- and likewise-circulating vortices are randomly placed in a circle of radius 10ξ centered at the location of each lattice site, with an enforced minimum separation of ξ between vortices. This closely reproduces configurations observed during disintegration of $\kappa_i = \pm 6$ vortices in the dPGPE after short times. Because of the interaction between compressible degrees of freedom and dissipation in the decay of a $\kappa_i = \pm 6$ vortex in the dPGPE, the timescales over which the initially separated groups of vortices mix are not completely consistent between the dPGPE and the point-vortex model (that does not include these effects). For $\gamma = 10^{-1}$ the dPGPE exhibits faster mixing, while for $\gamma = 10^{-5}$ the point-vortex model mixes faster. However, once the initial clusters have mixed, and the vortices become well-separated,

the point-vortex and dPGPE vortex dynamics become similar in all cases (a–c) [20].

The incompressible kinetic energy spectrum of our point-vortex model can be written analytically in terms of the vortex positions, an approach pioneered by Novikov [33] for the pure point-vortex model. Describing quantum vortex cores by the ansatz $\psi(\mathbf{r}-\mathbf{r}_i, \phi) = n_0[r^2/(r^2+\xi^2\Lambda^{-2})]^{1/2}e^{i\kappa_i\phi}$, where n_0 is the background homogeneous superfluid density and $\Lambda \approx 0.825$ [12], in the periodic square box of length $L\xi$ the incompressible kinetic energy spectrum is [5]

$$\frac{E^i(\mathbf{k})}{N} = G_\Lambda(k\xi) \left[1 + \frac{2}{N} \sum_{i=1}^{N-1} \sum_{j=i+1}^N \kappa_i \kappa_j \cos(\mathbf{k} \cdot \mathbf{r}_{ij}) \right], \quad (6)$$

where $G_\Lambda(k\xi) = \Omega_0 \xi^4 g(k\xi/\Lambda)/(\pi\Lambda k\xi)$, $\Omega_0 = \pi\hbar^2 n_0/m\xi^2$ is the quantum of enstrophy, $g(z) = (z/4)[I_1(z/2)K_0(z/2) - I_0(z/2)K_1(z/2)]^2$ (for modified Bessel functions I_α and K_α), and the momentum $\mathbf{k} = (n_x\Delta k, n_y\Delta k)$, for $\Delta k = 2\pi/L\xi$ and $n_x, n_y \in \mathbb{Z}$. As established previously [12], Eq. (6) leads to an angularly-integrated kinetic energy spectrum, $E^i(k) = k \int_0^{2\pi} E^i(\mathbf{k}) d\phi_k$, that exactly obeys the universal power-law $E^i(k) = C(k\xi)^{-3}$ in the ultraviolet ($k \gg \xi^{-1}$), where $C = N\Lambda^2\Omega_0\xi^3$ and $k = |\mathbf{k}|$. In the infrared ($k \lesssim \xi^{-1}$) the spectrum of randomly distributed vortices obeys the power-law $E^i(k) = C(k\xi)^{-1}/\Lambda^2$.

In order to study spectral energy transport in our model, we consider the *transfer function* of classical turbulence, $T(\mathbf{k}) = dE^i(\mathbf{k})/dt$ [2], given by

$$T(\mathbf{k}) = -2G_\Lambda(k\xi) \sum_{i=1}^{N-1} \sum_{j=i+1}^N \kappa_i \kappa_j \sin(\mathbf{k} \cdot \mathbf{r}_{ij}) \mathbf{k} \cdot \left(\frac{d\mathbf{r}_i}{dt} - \frac{d\mathbf{r}_j}{dt} \right), \quad (7)$$

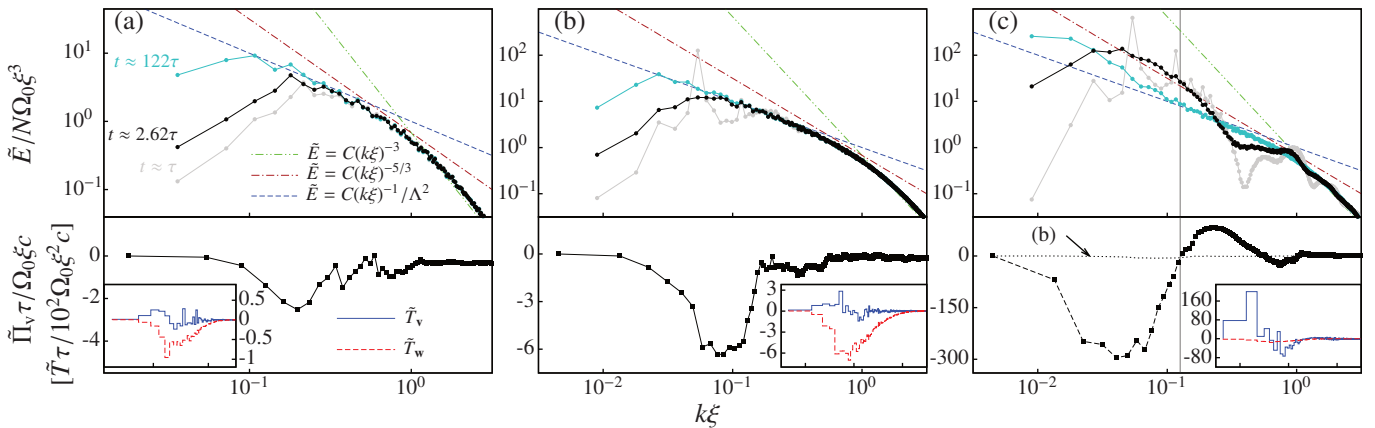


FIG. 2. (Color online) Spectral energy transport in the phenomenological point-vortex model (see also supplementary movies [20]): For the parameters given in Fig. 1, (a–c) show ensemble and time-averaged incompressible energy spectrum (top), flux (bottom), and transfer function (bottom, inset). Straight lines show the universal ultraviolet spectrum $\tilde{E} = C(k\xi)^{-3}$ and the infrared spectrum for randomly distributed vortices $\tilde{E} = C(k\xi)^{-1}/\Lambda^2$ (see text). A Kolmogorov scaling law $\tilde{E} = C(k\xi)^{-5/3}$ is also shown for reference. Time derivatives are scaled to the turnover time τ (see text) and time averaging is done over a window of duration 0.63τ [0.75 τ] in (a) [(b,c)], centered as indicated. Transfer functions and fluxes are shown for time $t \approx 2.62\tau$. Vertical lines in (c) indicate the transition from negative to positive flux. The spectrum and flux in case (c) are broadly consistent with results expected for classical decaying turbulence [19].

where the vortex velocities are known from Eq. (3). One can split $T(\mathbf{k})$ into Hamiltonian and dissipative parts $T(\mathbf{k}) = T_v(\mathbf{k}) + T_w(\mathbf{k})$, where

$$T_u(\mathbf{k}) = -2G_\Lambda(k\xi) \sum_{i=1}^{N-1} \sum_{j=i+1}^N \kappa_i \kappa_j \sin(\mathbf{k} \cdot \mathbf{r}_{ij}) \mathbf{k} \cdot (\mathbf{u}_i - \mathbf{u}_j), \quad (8)$$

for $\mathbf{u} = \{\mathbf{v}, \mathbf{w}\}$. Since we are interested in spectral energy transport at large scales, which may be strongly influenced by the box size in negative temperature states [24], we avoid approximating the angularly-integrated transfer function $T(k) = \int_0^{2\pi} T(\mathbf{k}) k d\phi_k$ analytically. Instead we introduce the discrete transfer function for $n = 1, 2, \dots$

$$\tilde{T}(n\Delta k) = \sum_{(n-\frac{1}{2})\Delta k < |\mathbf{k}| \leq (n+\frac{1}{2})\Delta k} T(\mathbf{k}) \Delta k, \quad (9)$$

that measures the rate of change of energy in the wavenumber range specified in the sum. From Eq. (9) we may define the discrete flux for $n = 0, 1, \dots$

$$\tilde{\Pi}[(n+1/2)\Delta k] = - \sum_{m=1}^n \tilde{T}(m, \Delta k) \Delta k. \quad (10)$$

For $\gamma = 0$, this defines the instantaneous energy flux through the k -space surface $|\mathbf{k}| = (n + \frac{1}{2})\Delta k$ ¹. In the presence of dissipation the meaning of $\tilde{\Pi}[(n+1/2)\Delta k]$ is not clear. However, crucially, the partition of $T(\mathbf{k})$ into Hamiltonian and dissipative parts [Eq. (8)] carries over naturally to $\tilde{T}(n\Delta k)$ and

$\tilde{\Pi}[(n+1/2)\Delta k]$. Hence, we are able to define three important quantities; $\tilde{T}_v(n\Delta k)$, the change in energy due to energy transport to or from other scales; $\tilde{T}_w(n\Delta k)$, the change in energy due to dissipative losses; and $\tilde{\Pi}_v[(n+1/2)\Delta k]$, the energy flux ignoring dissipative losses.

Numerically, evaluation of \tilde{T}_v , \tilde{T}_w , and $\tilde{\Pi}_v$ up to and beyond the vortex core momentum scale ($k \sim \xi^{-1}$) is expensive for large N and large L . To overcome this numerical challenge we developed GPU codes [34] that allow us to evaluate these quantities for many vortex configurations ($\sim 10^4$) within a reasonable timeframe. When suitably averaged over time and ensemble, in analogy to studies of classical turbulence [19], these quantities offer a detailed picture of spectral energy transport in our point-vortex model.

V. RESULTS AND DISCUSSION

Figure 2 and the supplementary movies [20] provide support our previous classification of the regimes of 2DQT, presented in Fig. 1, and provide quantitative confirmation of the nature of spectral energy transport in cases (a–c).

In the strongly dissipative cases [Fig. 2(a,b)] the relative magnitude of \tilde{T}_v and \tilde{T}_w are comparable, highlighting the key role of dissipation in this regime. The absence of any lossless inertial range rules out the existence of a turbulent cascade. Instead the spectrum undergoes a dissipative collapse: the total kinetic energy and the vortex number decrease rapidly, with little energy transport occurring. Note that we plot the kinetic energy spectrum $\tilde{E}(k)$ divided by the average number of vortices N in [Fig. 2] and the supplementary movies, in order to clearly show the spectrum as a function of k at all times. This can create the impression of a transfer of energy towards low k during the time-development of our plots of the spectrum; however, this is caused by the fact that both dissipation and

¹ This becomes equal to the conventional continuum flux $\Pi(k) = - \int_0^k T(k') dk'$ in the high- k limit, by setting $k = (n + \frac{1}{2})\Delta k$.

vortex annihilation remove energy preferentially at high k . As indicated by the plots of \bar{T}_v , \bar{T}_w , and $\bar{\Pi}_v$, the actual transfer of energy to large scales due to vortex interactions is not significant.

For the case of hydrodynamic vortex turbulence [Fig. 2(c)], dissipation is not significant. The spectrum and flux resemble those of classical decaying 2D turbulence generated from a similar initial concentration of energy, where a transient dual energy-ensrophy cascade is observed [19]. While the scale ranges are small (as expected for a system of a few hundred vortices when compared to classical turbulence), the spectrum does show some respective $k^{-5/3}$ and k^{-3} character above and below the scale of the transition from negative to positive flux (vertical line), suggesting that a quasi-classical dual energy-ensrophy cascade may be an emergent phenomenon in large-scale 2DQT.

A potentially powerful feature of our point-vortex model, due to its phenomenological treatment of effects below the vortex core scale, is that it may also be useful to describe the large-scale behaviour of vortices in other superfluids with different microscopic vortex core structure. For instance, as we describe in detail in Appendix A, we suspect the regime of dissipative collapse [Fig. 2(a,b)] may describe aspects of the holographic superfluid investigated in Ref. [7], in which a direct cascade of energy was previously inferred. This offers a possible resolution of the apparent conflict between Ref. [7] and Refs. [4–6] over the direction of energy transport in decaying 2DQT.

VI. CONCLUSIONS

Firstly, we used the damped, projected Gross–Pitaevskii equation (dPGPE) to examine several regimes of decaying 2DQT resulting from an unstable lattice-type initial condition. By varying the system size and the dissipation rate we showed the existence of at least three regimes: dissipative dipole gas, strong wave turbulence, and hydrodynamic vortex turbulence. These findings help to clarify the relation between previous studies of decaying 2DQT that have examined systems from different regimes.

Secondly, we introduced a phenomenological point-vortex model that accurately describes the vortex dynamics of decaying 2DQT in most cases (excepting the case of strong wave turbulence). We have used this model to elucidate the nature of spectral energy transport due to quantum vortex dynamics. We find that significant spectral energy transport due to vortex interactions occurs only for large systems subject to weak dissipation, and that in this case kinetic energy is transported to large scales. Our results for both energy spectra and energy fluxes provide some indication that a transient dual energy-ensrophy cascade, analogous to that present in the decay of turbulence in a classical fluid, may emerge in large-scale 2DQT. Future work will focus on understanding this emergent phenomenon in both forced and decaying turbulence.

ACKNOWLEDGMENTS

We thank B. P. Anderson, S. A. Gardiner, and R. Gregory for valuable discussions. We are grateful to P. M. Chesler and A. Lucas for discussions regarding Ref. [37]. This work was supported by The New Zealand Marsden Fund, and a Rutherford Discovery Fellowship of the Royal Society of New Zealand (ASB). TPB was partly supported by the UK EPSRC (EP/K030558/1). We acknowledge the NZ eScience Infrastructure (<http://www.nesi.org.nz>) and the University of Otago for providing access to Nvidia Tesla GPUs.

Appendix A: CONNECTIONS TO HOLOGRAPHIC SUPERFLUIDS

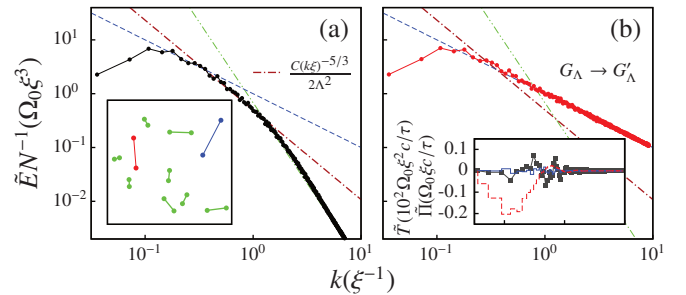


FIG. 3. (Color online) Accidental Kolmogorov $k^{-5/3}$ -scaling close to the vortex-core crossover: In (a), ensemble averaging over quiescent, non-turbulent, low-energy configurations of 20 vortices consisting mostly of vortex dipoles ($L = 175$, example inset) yields an appreciable apparent $k^{-5/3}$ -scaling region directly connected to the k^{-3} vortex-core scaling. In (b), analytically removing the vortex-core scaling destroys this $k^{-5/3}$ region, which for $\gamma = 10^{-1}$ is clearly not related to a lossless inertial range (see inset). Curves as in Fig. 2 of the main text.

In the main text, we have considered decaying two-dimensional quantum turbulence in a compressible superfluid described by a Gross–Pitaevskii model. Our results show that in vortex-dominated regimes where sound energy is negligible [our cases (a), (b), and (c)] one observes either dissipative collapse of the spectrum [strong dissipation, cases (a), (b)] or transport of energy to large scales [weak dissipation, case (c)]. One question prompted by these results is how they may be connected to turbulence in holographic 2D superfluids [7, 35, 36] for which a direct cascade of energy was recently inferred in [7].

A problem in connecting our results and those of Ref. [7] is that, unlike the Gross–Pitaevskii description, holographic superfluids are not explicitly constructed to describe experimental atomic superfluids. Indeed, the structure of vortex cores in holographic superfluids has been shown to be different from the Gross–Pitaevskii form [36]. Nonetheless, we note that movies [20] of the dPGPE evolution in case (a) of our work are very similar to the movies of holographic superfluid vortex dynamics in Ref. [7]. In particular, both exhibit strong damping of sound waves, rapid vortex-antivortex anni-

hilation, and evolution towards a positive-temperature vortex configuration. This similarity suggests that the holographic superfluid in Ref. [7] probes a regime of small system size (relative to the vortex core) with dissipation several orders of magnitude stronger than realized in atomic BEC experiments — where typically $\gamma \sim 10^{-5} - 10^{-4}$ [12]. The possibility of describing the holographic superfluid of Ref. [7] using a point-vortex model with large dissipation was also recently pointed out elsewhere [37]. If such a description is appropriate then, according to our results, one would anticipate a dissipative collapse of the spectrum in the scenario of Ref. [7], rather than a $k^{-5/3}$ spectrum and a direct cascade of energy.

Despite the possibility of significant differences between Gross-Pitaevskii-like and holographic superfluids, for a state with negligible density fluctuations outside of the vortex cores, the kinetic energy spectra of Gross-Pitaevskii-like and holographic superfluids should in fact be very similar on physical grounds. In particular, in the ultraviolet the linear scaling of the wavefunction at the vortex core in both superfluids [36] yields a k^{-3} spectrum, while in the infra-red both systems must recover a configurational point-vortex spectrum. Thus, differences between the Gross-Pitaevskii and holographic kinetic energy spectra should be confined to the crossover region ($k \sim \xi^{-1}$). Consequently, a $k^{-5/3}$ spectrum in the configurational spectrum of a holographic superfluid should be understandable in terms of a point-vortex model.

In Fig. 3(a) we show the average incompressible kinetic energy spectrum of 1000 random neutral 20-vortex configurations with point-vortex energy (per vortex) ≈ -1 (see

Ref. [5]). Such configurations [example inset in Fig. 3(a)], which do not correspond to classical fluid turbulence [24], resemble configurations obtained in case (a) and Ref. [7] after most vortices have been annihilated in a dissipative collapse. Nonetheless, the average spectrum exhibits a roughly half-decade sized region with apparent $k^{-5/3}$ scaling [Fig. 3(a)]. However, replacing $G_\Lambda(k\xi) \rightarrow G'_\Lambda(k\xi) = \Omega_0 \xi^4 / \pi (k\xi)^2$ allows recovery of the pure point-vortex spectrum [Fig. 3(b)] for the same vortex configuration [12]. This spectrum follows the single-vortex k^{-1} scaling throughout the apparent $k^{-5/3}$ region in Fig. 3(a), showing that the latter is due to the vortex core structure (contained in G_Λ) and is unrelated to vortex interactions and turbulence. Consistent with this picture, the ensemble-averaged transfer function and incompressible energy flux [inset in Fig. 3(b)] show no lossless inertial range.

While the vortex core structure in a holographic superfluid may be different in its details, it quite likely leads to a similar “accidental” $k^{-5/3}$ scaling. This offers an alternative explanation for the $k^{-5/3}$ scaling in the spectrum attributed to a direct cascade in Ref. [7]. An intriguing question that arises is whether adjusting parameters in the holographic description might yield a regime of weakly-dissipative holographic superfluid behaviour similar to our case (c), recovering the statistical transport of energy to large scales associated with classical 2D turbulence. Recent work [37] has suggested a positive answer to this question by analogy to a weakly-dissipative point-vortex model, but this has not presently been confirmed by direct simulation of a weakly-dissipative holographic superfluid. Directly addressing this question may help to further elucidate the physical nature of holographic superfluids.

-
- [1] R. H. Kraichnan and D. Montgomery, *Rep. Prog. Phys.* **43**, 547 (1980).
- [2] M. Lesieur, *Turbulence in Fluids*, 4th ed. (Kluwer Academic Publishers, Netherlands, 1990).
- [3] T. W. Neely, A. S. Bradley, E. C. Samson, S. J. Rooney, E. M. Wright, K. J. H. Law, R. Carretero-González, P. G. Kevrekidis, M. J. Davis, and B. P. Anderson, *Phys. Rev. Lett.* **111**, 235301 (2013).
- [4] M. T. Reeves, T. P. Billam, B. P. Anderson, and A. S. Bradley, *Phys. Rev. Lett.* **110**, 104501 (2013).
- [5] T. P. Billam, M. T. Reeves, B. P. Anderson, and A. S. Bradley, *Phys. Rev. Lett.* **112**, 145301 (2014).
- [6] T. Simula, M. J. Davis, and K. Helmersson, *Phys. Rev. Lett.* **113**, 165302 (2014).
- [7] P. M. Chesler, H. Liu, and A. Adams, *Science* **341**, 368 (2013).
- [8] R. Numasato, M. Tsubota, and V. S. L'vov, *Phys. Rev. A* **81**, 063630 (2010).
- [9] D. Proment, S. Nazarenko, and M. Onorato, *Phys. Rev. A* **80**, 051603 (2009).
- [10] S. Nazarenko and M. Onorato, *Physica D* **219**, 1 (2006).
- [11] S. Nazarenko and M. Onorato, *J. Low Temp. Phys.* **146**, 31 (2007).
- [12] A. S. Bradley and B. P. Anderson, *Phys. Rev. X* **2**, 041001 (2012).
- [13] M. T. Reeves, B. P. Anderson, and A. S. Bradley, *Phys. Rev. A* **86**, 053621 (2012).
- [14] B. Nowak, D. Sexty, and T. Gasenzer, *Phys. Rev. B* **84**, 020506 (2011).
- [15] B. Nowak, J. Schole, D. Sexty, and T. Gasenzer, *Phys. Rev. A* **85**, 043627 (2012).
- [16] J. Schole, B. Nowak, and T. Gasenzer, *Phys. Rev. A* **86**, 013624 (2012).
- [17] R. Numasato and M. Tsubota, *J. Low Temp. Phys.* **158**, 415 (2010).
- [18] P. B. Blakie, A. S. Bradley, M. J. Davis, R. J. Ballagh, and C. W. Gardiner, *Adv. in Phys.* **57**, 363 (2008).
- [19] P. D. Mininni and A. Pouquet, *Phys. Rev. E* **87**, 033002 (2013).
- [20] See Supplemental Material, available at [URL], for movies of the dPGPE evolution shown in Fig. 1 and the point-vortex model evolution shown in Fig. 2.
- [21] P. B. Blakie, *Phys. Rev. E* **78**, 026704 (2008).
- [22] S. J. Rooney, T. W. Neely, B. P. Anderson, and A. S. Bradley, *Phys. Rev. A* **88**, 063620 (2013).
- [23] G. W. Stagg, A. J. Allen, N. G. Parker, and C. F. Barenghi, (2014), [arXiv:1408.3268](https://arxiv.org/abs/1408.3268).
- [24] L. Campbell and K. O'Neil, *Journal of Statistical Physics* **65**, 495 (1991).
- [25] M. T. Reeves, T. P. Billam, B. P. Anderson, and A. S. Bradley, *Phys. Rev. A* **89**, 053631 (2014).
- [26] A. L. Fetter, *Phys. Rev.* **151**, 100 (1966).
- [27] O. Törnkvist and E. Schröder, *Phys. Rev. Lett.* **78**, 1908 (1997).
- [28] M. Peach and J. S. Koehler, *Phys. Rev.* **80**, 436 (1950).
- [29] J. B. Weiss and J. C. McWilliams, *Physics of Fluids A: Fluid Dynamics* **3**, 835 (1991).

- [30] W. J. Kwon, G. Moon, J. Choi, S. W. Seo, and Y. Shin, (2014), [arXiv:1403.4658](#).
- [31] L. Pismen, *Vortices in Nonlinear Fields*, International series of monographs on physics (Clarendon Press, Oxford, 1999).
- [32] W. F. Vinen, *Phys. Rev. B* **64**, 134520 (2001).
- [33] E. A. Novikov, *Zh. Eksp. Teor. Fiz.* **68**, 1868 (1975), [*Sov. Phys. JETP* **41**, 937 (1975)].
- [34] NVIDIA Corporation, “[NVIDIA CUDA Programming Guide, Version 6.5](#),” (2014).
- [35] C. P. Herzog, P. K. Kovtun, and D. T. Son, *Phys. Rev. D* **79**, 066002 (2009).
- [36] V. Keränen, E. Keski-Vakkuri, S. Nowling, and K. P. Yogendran, *Phys. Rev. D* **81**, 126012 (2010).
- [37] P. M. Chesler and A. Lucas, (2014), [arXiv:1411.2610](#).